

Strong projectile-dependent forward-backward asymmetry of electron ejection by swift heavy ions in solids

H. Rothard,* M. Jung,† M. Caron, J.-P. Grandin, B. Gervais, A. Billebaud,‡ A. Clouvas,§ and R. Wünsch||
*Centre Interdisciplinaire de Recherches avec les Ions Lourds (CIRIL), Laboratoire Mixte CEA-CNRS UMR 11, Boîte Postale 5133,
 Rue Claude Bloch, F-14070 Caen Cedex 05, France*

(Received 7 October 1997)

We studied forward and backward electron ejection from carbon foils penetrated by swift ions (energy range, 20 keV/nucleon–74 MeV/nucleon; projectiles, H–U) over four orders of magnitude of electronic energy loss (0.01–25 keV/nm). Ejection of fast electrons from primary ionization and subsequent energy dissipation by secondary cascades are found to be asymmetric. Electronic energy deposition by swift ions is thus different at the entrance surface, in the solid's bulk, and at the exit surface. The effect strongly increases with projectile atomic number due to an increasing contribution of close collisions and enhanced fast-electron ejection. [S1050-2947(98)06205-2]

PACS number(s): 79.20.Rf, 34.50.Dy, 61.80.Jh

I. INTRODUCTION

A typical feature of swift heavy ions is their high electronic energy loss per unit path length dE/dx , and strong perturbation of the solid due to the huge induced density of deposited energy up to some tens of keV per nm. Typically, hundreds or thousands of electrons are excited per nm along the ion trajectory for a typical track diameter of some tens of nm. As a consequence of electronic energy loss, strongly ionizing high-velocity particles such as heavy ions (or cluster) can create specific damage and lead to track formation in solids [1]. The first step of such irradiation effects consists in ionization, i.e., the ejection of electrons and their subsequent transport through the solid. In this way, the deposited energy is transported and distributed away from, but along, the ion track. A fraction of these electrons is ejected from the solid surface and kinetic electron emission is thus an important basic probe for the interaction of swift heavy ions with solids [2–5], and contributes to the understanding of radiation effects in solids. In this paper, we report on evidence from electron yield measurements that primary ionization and energy transport by fast electrons and subsequent secondary electron cascade are strongly nonisotropic. The effect increases with energy and projectile atomic number. This has the consequence that electronic energy deposition by swift

ions is different at the entrance surface, in the bulk of the solid, and the exit surface.

Since the observed effects are due to electronic excitations, the electronic energy loss per unit path length dE/dx immediately comes to mind as the first choice of an appropriate scaling parameter for energy deposition and secondary particle emission. Consequently, it is often assumed that electron yields γ_i (the mean number of emitted electrons per incoming projectile) are proportional to the electronic energy loss per unit path length dE/dx [2–4]. It is a common practice [3,4,6] to compare electron yields to dE/dx by defining a ratio

$$\Lambda_i(Z_P, v_P) = \gamma_i / (dE/dx). \quad (1)$$

The index i stands for B , F , or T if backward (from the beam-entrance side), forward (the beam-exit side), or total electron yields are concerned ($\gamma_T = \gamma_F + \gamma_B$). In practice, $dE/d(\rho x)$ measured in keV/($\mu\text{g}/\text{cm}^2$) rather than dE/dx is used and tabulated [7].

It has long been known that backward electron yields [4] and total electron yields from both surfaces of the foil targets [6] show a pronounced dependence on the projectile atomic number Z_P (for a review, see Ref. [4]). Recently, the projectile dependence of backward and forward electron emission from thin foils has been studied by several groups [8–10] at low-projectile velocities around or below the maximum of the electronic energy-loss curve. This velocity region is particularly “tricky” because of pre-equilibrium effects connected to charge-exchange and penetration-depth-dependent energy loss. Both ionic charge and dE/dx evolve into a layer beyond the surface comparable to the escape depth of slow electrons [5,6]. Also, the slowing down of the projectiles in the target cannot be neglected even for the thinnest foils, so that the velocity and dE/dx are different for the incoming and the outgoing beam. This makes the interpretation of such measurements difficult. However, in general, a reduction of Λ_i (for both backward and forward yields) with increasing projectile atomic number Z_P (possibly with a superposed oscillatory structure) has been observed: $\Lambda_i(Z_P > 1) < \Lambda_i(Z_P = 1)$. It is interesting to note that similar results have been

*Author to whom correspondence should be addressed.
 FAX: +33 (0) 2 31 45 47 14.

Electronic address: ROTHARD@GANIL.FR

†Present address: ATOMIKA Instruments GmbH, Bruckmannring 40, D-85764 Oberschleissheim, Germany.

‡Present address: Institut des Sciences Nucléaires, IN2P3-CNRS/ Université J. Fourier, 53 Avenue des Martyrs, F-38026 Grenoble Cedex, France.

§Permanent address: Department of Electrical and Computer Engineering, Aristotelian University, GR-54006 Thessaloniki, Greece.

||Permanent address: Institut für Kernphysik der J.-W. Goethe Universität, August-Euler-Strasse 6, D-60486 Frankfurt am Main, Germany.

obtained for swift cluster impact [11,12] as a function of cluster size n (instead of atomic number). For example, for H_n^+ impact on thin carbon foils, it was found that $\Lambda_i(n>1) < \Lambda_i(n=1)$ [11].

Here we present a comprehensive experimental study of the projectile and the velocity dependence of backward (γ_B) and forward (γ_F) electron yields of carbon foils penetrated by swift ions. We studied the relationship of electron yields and energy deposition in a wide energy range (from 20 keV/nucleon up to 74 MeV/nucleon). This allows us to study the dependence of electron emission on the projectile atomic number at high velocities (around 10 MeV/nucleon, above the maximum of the electronic energy-loss curve) for a large set of projectiles (from protons up to uranium: H, He, Li, Be, C, Mg, Ar, Cr, Ni, Cu, Cd, Te, Pb, and U). This way, four orders of magnitude of electronic energy loss are covered (from ~ 0.01 to 25 keV/nm).

II. EXPERIMENT AND TARGET THICKNESS DEPENDENCE

Most of the data presented have been obtained at the Grand Accélérateur National d'Ions Lourds (GANIL) in Caen, France; some data are from Institut für Kernphysik (Frankfurt), Institut de Physique Nucléaire (Lyon), and Institute of Nuclear Physics, NCSR Demokritos (Athens). We used carbon foils of different thicknesses (typically 20 to 7000 $\mu\text{g}/\text{cm}^2$, approximately 0.1 to 35 μm) in a standard vacuum ($p \approx 5 \times 10^{-7}$ mbar). All foils used were manufactured at IPN, Lyon to obtain comparable and reproducible results at the different accelerators [9,11,13–16]. The experimental setup and procedures for the electron-yield measurements have been described in Refs. [9,15,16]. It is important to note that the charge states q of the incoming ions were chosen close to the mean final charge $\langle q_f \rangle$ in order to prevent the above-mentioned pre-equilibrium effects [5,6,15]. Also, the foils are so thin that the change of ion energy within the foils can be neglected.

In the following, we distinguish between “thick” and “thin” foil targets. In order to explain the meaning of these terms, we show the target thickness dependence of electron yields for swift ions (C at 11.1 MeV/nucleon and Cu at 9.6 MeV/nucleon) in Fig. 1. The term “thick targets” refers to foils for which forward and backward yields have reached constant values and do not evolve further with target thickness. This thickness depends on the range of the fast electrons and thus on the projectile velocity (at 10 MeV/nucleon, $\sim 500 \mu\text{g}/\text{cm}^2$). For “thin targets,” only the backward yield has reached a constant value. In contrast, the secondary electron cascade due to fast electrons (mainly in the forward direction) from primary ionization and the target thickness dependence of forward yields just begin to start. At 10 MeV/nucleon, as can be seen from Fig. 1, this is the case around 20 $\mu\text{g}/\text{cm}^2$. A thorough discussion of the target thickness dependence of ion-induced electron yields can be found in Ref. [16].

III. RESULTS: VELOCITY AND PROJECTILE DEPENDENCE

The dependence of the ratios Eq. (1) for protons, carbon ions, and nickel (copper) ions is shown in Fig. 2 for thick

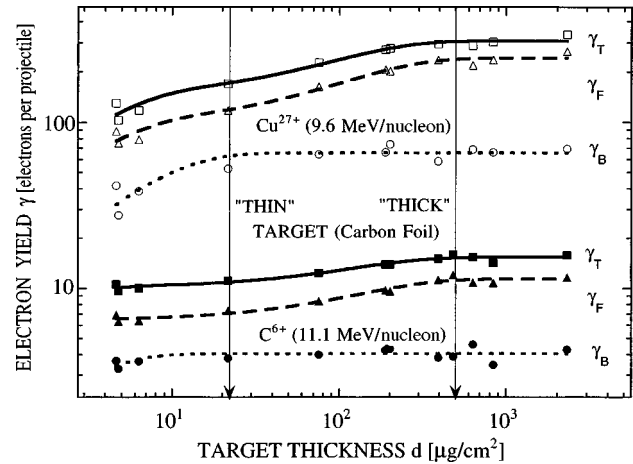


FIG. 1. Target-thickness dependence of backward (γ_B , from the beam entrance side), forward (γ_F , from the beam exit side), and total electron yields ($\gamma_T = \gamma_F + \gamma_B$) for swift C and Cu ions (~ 10 MeV/nucleon as indicated).

targets. For proton impact, within error bars, the ratio is constant over the whole investigated energy range (0.02–7.5 MeV/nucleon) for both forward and backward yields. In the particular case of proton impact, the above-mentioned assumption is correct and electron emission yields are propor-

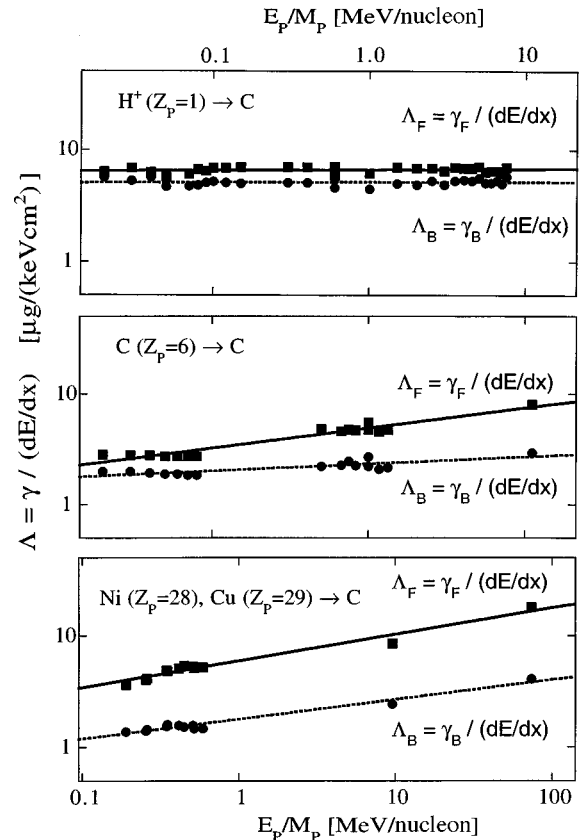


FIG. 2. The ratios of electron yields and electronic energy loss per unit path length $\Lambda_i(E/M) = \gamma_i / (dE/dx)$ as a function of the projectile energy E/M for protons, carbon ions, and nickel (copper) ions (as indicated). The index i stands for either B (backward emission) or F (forward emission). The lines are fits of a power law $\Lambda_i = C_i(E/M)^{n_i}$ to the data.

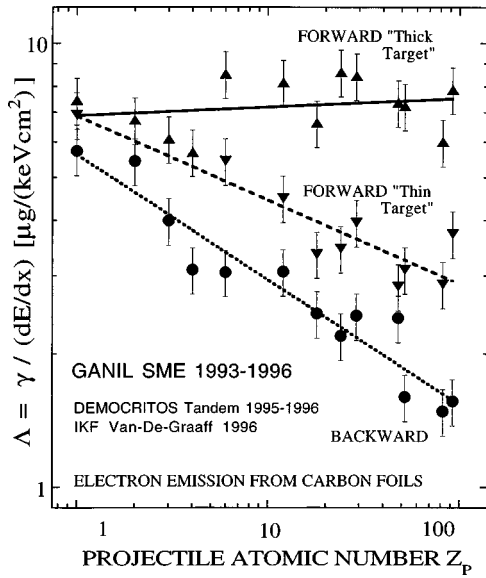


FIG. 3. Ratios of electron yields and electronic energy loss per unit path length $\Lambda_i(Z_p) = \gamma_i / (dE/dx)$ as a function of the projectile atomic number Z_p . Only data around 10 MeV/nucleon ($E = 3.8\text{--}13.6$ MeV/nucleon) have been included. Triangles, forward yields obtained with “thick targets;” upside down triangles, forward yields obtained with “thin targets;” circles, backward yields (see text). The lines represent a power law $\Lambda_i = c_i(Z_p)^{n_i}$.

tional to dE/dx . In contrast, for C ions, a slight increase is observed (0.2–9.6 MeV/nucleon). For the heavy Cu and Ni ions, the increase of Λ_i with energy is more pronounced (0.2 to 74 MeV/nucleon). The increase is stronger for forward rather than for backward yields. The energy dependence of Λ_i can be described by a power law:

$$\Lambda_i = C_i(E/M)^{n_i}. \quad (2)$$

The solid lines in Fig. 2 are fits of Eq. (2) to the experimental data. We obtain $n_B = 0.003, 0.064,$ and 0.18 for backward emission, and $n_F = 0.007, 0.18,$ and 0.24 for forward emission for H, C, and Cu/Ni projectiles, respectively.

Now we can study the projectile dependence for approximately constant velocity. The corresponding ratios $\Lambda_i(Z_p) = \gamma_i / (dE/dx)$ are shown in Fig. 3 as a function of the projectile atomic number Z_p . Only medium energy data around 10 MeV/nucleon ($E = 3.8\text{--}13.6$ MeV/nucleon) have been included [17]. The lines again represent a power law $\Lambda_i = c_i(Z_p)^{n_i}$. The values of the exponent are $n_F = 0.019$ for forward yields obtained with thick targets, $n_f = -0.19$ for forward yields obtained with thin targets, and $n_B = -0.28$ for backward yields. One observes that $\Lambda_B(Z_p)$ for backward yields and $\Lambda_F(Z_p)$ for forward yields from thin targets strongly decrease with Z_p . In contrast, $\Lambda_F(Z_p)$ is approximately constant for forward yields with thick targets. The ratio of forward to backward yields $R = \gamma_F / \gamma_B$ from thick targets strongly increases with the projectile atomic number from $\sim R = 1.2$ for protons up to $R = 5$ for the heaviest ions.

IV. DISCUSSION

An explanation lies in preferential fast electron ejection and energy deposition in forward direction. The “fast elec-

trons” (say, of energies of at least some hundred eV), with large mean free path and range, carry away a part of the deposited energy from the entrance surface region. Consequently, more energy is deposited far away from the entrance surface, deep into the bulk. This leads to reduced electron emission in the backward direction, but leads to enhanced slow electron ejection in fast-electron-induced secondary electron cascades in the forward direction. For thin targets, the fast electrons cannot deposit all of their energy within the solid. A large number of them leave the solid without secondary interaction or without contributing significantly to the secondary electron cascade. This can clearly be seen from the thin target curve for forward emission of Fig. 3, which is close to the backward curve even in absolute value. On the other hand, the energy that seems to be missing in the backward direction can be found in forward emission if the target is thick enough to allow fast electrons, originating from the first layers of the beam entrance side to deposit their energy within the solid close to the exit surface.

A particularly interesting result is that this effect of preferential forward projection of energy deposition increases with Z_p , as can be seen from the increasing ratio R of forward to backward emission (Fig. 3). This can be explained as follows. Close, violent collisions and thus high-energy electron emission may be favored with increasing projectile atomic number. Consequently, the emission of fast electrons is enhanced; a relative reduction of low-energy electron emission and possibly plasmon excitation occurs. The mean energy $\langle E \rangle$ of electrons is increased [16,18,19]. This leads to a shift in the electron energy distribution toward higher energies for heavier and faster ions.

These arguments could also explain the stronger increase of forward emission compared to backward emission for heavy ions seen in Fig. 2 with increasing velocity. In this respect, it is important to note that for “medium heavy ions” (Z_p around 30), at 10 MeV/nucleon, about 20% of ejected electrons are fast electrons; this fraction increases up to about 35% at 74 MeV/nucleon [16]. At 8 MeV/nucleon, about 30% of ejected electrons are fast electrons for the heaviest projectiles (uranium) [19].

Available theoretical models (such as the numerical simulation we compared to target-thickness-dependent electron-yield measurements in Refs. [15,16]) indeed are not capable of explaining or reproducing the results. We will briefly discuss in the following some of the possible reasons. Electron emission can roughly be divided into three steps: (a) primary ionization of the target atoms, (b) electron migration through the solid (transport), and (c) transmission through the surface-potential barrier.

Specific effects connected to the high charge and strong perturbation induced by heavy multiply charged ions may occur at all of the above-mentioned steps.

(d) Primary ionization cross sections deviate from first-order theory (see, e.g., [20]), but in most numerical simulations first-order ionization or linear dielectric theory are used. This yields a simple q^2 or Z_p^2 scaling for fixed velocity. In contrast, if we plot the ratio of the measured total electron yields and the square of the projectile charge as a function of the projectile atomic number (Fig. 4, diamonds), we observe a decrease by a factor of 2 from $Z_p = 1$ to $Z_p = 48$. Available numerical simulation would yield a constant projectile inde-

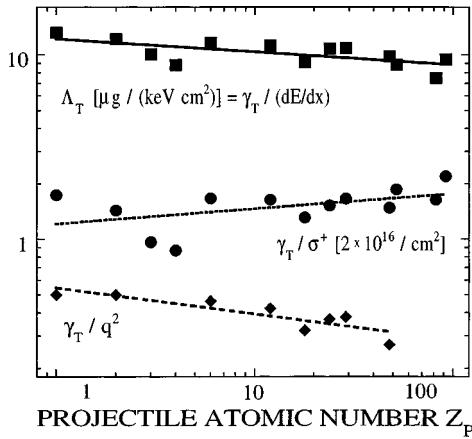


FIG. 4. Ratios of electron yields and the square of the charge of the projectiles γ/q^2 (diamonds), the ratios $\Lambda_T(Z_p) = \gamma/(dE/dx)$ of electron yields and electronic energy loss per unit path length (squares, from Fig. 3), and the ratio of electron yields and the total net target ionization cross-section γ/σ^+ (Eq. 3, Ref. [21], circles) as a function of the projectile atomic number Z_p . The lines (representing power laws in Z_p) are to guide the eye. For γ/q^2 (diamonds), electron yield data below 5 MeV/nucleon were skipped, and only data between 7.5 and 13.6 MeV/nucleon were extrapolated to the fixed velocity of 10 MeV/nucleon.

pendent value, i.e., a horizontal line in Fig. 4 and is thus off by a factor of 2.

“Reduced” electron yields related to deviations of the atomic-target ionization cross section from a simple q^2 scaling already occur in single atomic collisions (gas targets) [20,21]. To test whether such effects could already explain the observed decrease of electron yields with the square of the charge, we included, in Fig. 4, the ratios of electron yields and the total net-target ionization cross section γ/σ^+ (circles) for neutral target atoms bombarded with heavy ions of charge q . Such cross sections can be described by an empirical scaling rule [21]

$$\sigma^+ \approx q^2 K k \{1 - \exp[-1/(kq)]\}, \quad (3)$$

with $K \approx 0.25 \times 10^{-15}$ and $k = 0.23/E_p$ with the projectile energy E_p measured in units of MeV/nucleon. In order to find a good approximation for the carbon target atoms, we used the mean values of K and k for He and Ne target atoms [21].

As can be seen from Fig. 4, this scaling parameter works quite well, so that one could conclude that the reduction effect is already due to the less-effective primary ionization with heavy highly charged ions. Note that, although the ratios Λ_T of total electron yields γ_T and dE/dx slightly decrease with Z_p (as also shown in Fig. 4), the electronic energy loss dE/dx also turns out to be a good scaling

parameter. Probably, this is due to the fact that it already accounts for high charge effects via the effective charge used to calculate the dE/dx values [7].

(b) and (c) The transport and emission of electrons induced by weakly ionizing particles (electrons, protons) is reasonably well understood [22,23]. In this case, the above-mentioned steps (a), (b), and (c) can be regarded as independent. Nevertheless, the high ionization density could have an influence on the transport of electrons in the wake of highly ionizing particles, such as heavy ions. In a similar manner, it could lead to a change of the effective surface barrier in the vicinity of the heavy-ion track. It was indeed the initial motivation for this work to test theoretical predictions [24] of order-of-magnitude electron-yield reductions due to the trapping of slow electrons in the positively charged wake of the ions. This effect could not be confirmed in its predicted strength [25], but such a condensed-matter effect related to the induced track potential or a modification of the surface-potential barrier cannot be completely excluded (see also the discussions in Refs. [18] and [25]). Effects related to the high charge density, induced in the wake of the ions as discussed in Ref. [24], should increase with increasing charge and decreasing velocity (or, in other terms, increase with the perturbation parameter q/v). The opposite is observed in Fig. 2, concerning the velocity dependence.

We finally mention that until now, only a reduction of heavy-ion-induced electron yields compared to the proton case, i.e., a decrease of Λ with Z_p , has been reported as mentioned above. A closer look at Fig. 2 shows that even strongly enhanced forward electron emission can be expected for swift heavy ions (medium to high Z_p , up to about 100 MeV/nucleon) if it could be assumed that proton-induced yields remain proportional to dE/dx at energies above 10 MeV/nucleon. Experimental evidence that this is indeed the case was recently reported for protons up to 70 MeV/nucleon [26]. One may only speculate about what would happen if heavy atom clusters would be available at such energies, if such effects could even be stronger due to a collective interaction of constituents [11,12].

In conclusion, numerical models with refined treatment of primary ionization (deviations from first-order theory, multiple ionization), and also including collective solid-state effects (on transport or surface transmission) are needed.

ACKNOWLEDGMENTS

It is a pleasure to thank D. Lelièvre and V. Mouton (CIRIL) for technical assistance. We acknowledge support from the European Community under Contract No. CHGE-CT94-0056 (Human Capital and Mobility, “GANIL European Installation”). M.J. and M.C. acknowledge Ph.D. grants from the CEA and the region of “Basse Normandie.” A.C. and H.R. acknowledge travel support from the “Service Culturel et Scientifique” of the French embassy in Athens, Greece.

[1] Fundamental and applied aspects of swift heavy ion interaction with condensed matter are subject of the Proceedings of the Third International Conference on Swift Heavy Ions in Matter SHIM-95, edited by N. Angert, A. Bourret, J. P. Grandin [Nucl. Instrum. Methods **B107** (1996)].

[2] *Ionization Of Solids By Heavy Particles*, Vol. 306 of NATO Advanced Study Institute, edited by R. Baragiola (Plenum, New York, 1993).

[3] J. Schou, *Scanning Microsc.* **2**, 607 (1988).

[4] W. Hofer, *Scanning Microsc. Suppl.* **4**, 265 (1990).

- [5] H. Rothard, *Scanning Microsc.* **9**, 1 (1995).
- [6] H. Rothard, J. Schou, and K. O. Groeneveld, *Phys. Rev. A* **45**, 1701 (1992).
- [7] J. F. Ziegler, J. P. Biersack, and U. Littmark, *The Stopping and Ranges of Ions in Matter* (Pergamon, New York, 1985), Vol. 1; F. Hubert, R. Bimbot, and H. Gauvin, *At. Data Nucl. Data Tables* **46**, 1 (1990).
- [8] A. M. Arrale, Z. Y. Zhao, J. F. Kirchoff, D. L. Weathers, F. D. McDaniel, and S. Matteson, *Phys. Rev. A* **55**, 1119 (1997).
- [9] A. Clouvas, C. Potiriadis, H. Rothard, D. Hofmann, R. Wünsch, K. O. Groeneveld, A. Katsanos, and A. C. Xenoulis, *Phys. Rev. B* **55**, 12086 (1997).
- [10] S. Gelfort, H. Kerkow, R. Stolle, V. P. Petukhov, and E. A. Romanowski, *Nucl. Instrum. Methods Phys. Res. B* **125**, 49 (1997).
- [11] H. Rothard, D. Dauvergne, M. Fallavier, K. O. Groeneveld, R. Kirsch, J. C. Poizat, J. Remillieux, and J. P. Thomas, *Radiat. Eff. Defects Solids* **126**, 373 (1992); A. Billebaud, D. Dauvergne, M. Fallavier, R. Kirsch, J. C. Poizat, J. Remillieux, H. Rothard, and J. P. Thomas, *Nucl. Instrum. Methods Phys. Res. B* **112**, 79 (1996).
- [12] K. Baudin, A. Brunelle, S. Della-Negra, J. Depauw, Y. Le-Beyec, and E. S. Parilis, *Nucl. Instrum. Methods Phys. Res. B* **117**, 47 (1996).
- [13] In particular, it is well known that electron yields from carbon foils depend on the accumulated ion fluence due to surface modification [14]. They decrease exponentially and tend towards an equilibrium value. Therefore, we irradiated the foils until electron yields reached the constant high fluence value.
- [14] H. Rothard, M. Jung, B. Gervais, J. P. Grandin, A. Billebaud, and R. Wünsch, *Nucl. Instrum. Methods Phys. Res. B* **107**, 108 (1996).
- [15] H. Rothard, C. Caraby, A. Cassimi, B. Gervais, J. P. Grandin, P. Jardin, M. Jung, A. Billebaud, M. Chevallier, K. O. Groeneveld, and R. Maier, *Phys. Rev. A* **51**, 3066 (1995).
- [16] M. Jung, H. Rothard, B. Gervais, J. P. Grandin, A. Clouvas, and R. Wünsch, *Phys. Rev. A* **54**, 4153 (1996).
- [17] The variation of Λ_i in the velocity range “around 10 MeV/nucleon” (from 4 to 13 MeV/nucleon) is small compared to the strong Z_p dependence of the ratios R of forward to backward electron yields (see Fig. 2) of up to a factor of 5 (less than 25% in the worst case shown in Fig. 1, Ni-Cu).
- [18] G. Schiwietz and G. Xiao, *Nucl. Instrum. Methods Phys. Res. B* **107**, 113 (1996).
- [19] G. Schiwietz, in *Ionization of Solids by Heavy Particles* (Ref. [2]), p. 197; see also: D. Schneider, G. Schiwietz, and D. DeWitt, *Phys. Rev. A* **47**, 3945 (1993).
- [20] P. D. Fainstein, V. H. Ponce, and R. D. Rivarola, *J. Phys. B* **21**, 287 (1988).
- [21] A. Cassimi, J. P. Grandin, L. H. Zhang, A. Gosselin, D. Hennecart, X. Husson, D. Leclerc, A. Lepoutre, and I. Lesteven-Vaisse, *Radiat. Eff. Defects Solids* **126**, 21 (1992).
- [22] A. Dubus, J.-C. Dehaes, J.-P. Ganachaud, A. Hafni, and M. Cailler, *Phys. Rev. B* **47**, 11056 (1993).
- [23] M. Caron, M. Beuve, H. Rothard, B. Gervais, A. Dubus, and M. Rösler, *Nucl. Instrum. Methods Phys. Res. B* **135**, 436 (1998).
- [24] J. E. Borovsky and D. M. Suszcynski, *Phys. Rev. A* **43**, 1433 (1991).
- [25] H. Rothard, M. Jung, J. P. Grandin, B. Gervais, M. Caron, A. Billebaud, A. Clouvas, R. Wünsch, C. Thierfelder, and K. O. Groeneveld, *Nucl. Instrum. Methods Phys. Res. B* **125**, 35 (1997).
- [26] C. M. Castaneda, L. McGarry, C. Cahill, and T. Essert, *Nucl. Instrum. Methods Phys. Res. B* **129**, 199 (1997).